BIOCHEMISTRY
including biophysical chemistry & molecular biology

Article

pubs.acs.org/biochemistry

Role of a Conserved Residue R780 in *Escherichia coli* Multidrug Transporter AcrB

Linliang Yu,[†] Wei Lu,[†] Cui Ye,[†] Zhaoshuai Wang,[†] Meng Zhong,[†] Qian Chai,[†] Michael Sheetz,[‡] and Yinan Wei*[,†]

[†]Department of Chemistry, University of Kentucky,Lexington, Kentucky 40506, United States

[‡]Center for Computational Sciences, University of Kentucky, Lexington, Kentucky 40506, United States

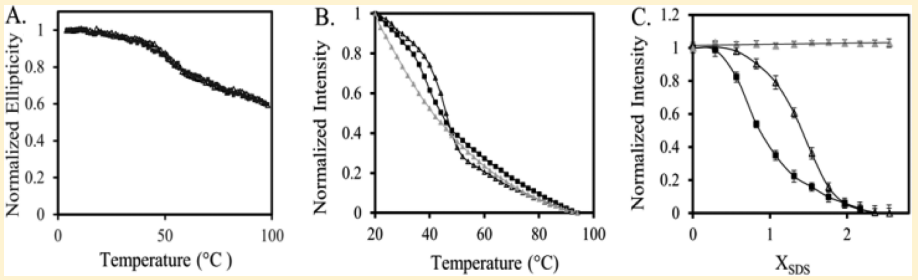

ABSTRACT: Multidrug efflux pumps play important roles in bacteria drug resistance. A major multidrug efflux system in Gram-negative bacteria is composed of the inner membrane transporter AcrB, outer membrane protein channel TolC, and membrane fusion protein AcrA. These three proteins form a large complex that spans both layers of cell membranes and the periplasmic space. AcrB exists and functions as a homotrimer. To identify residues at the trimer interface that play important roles in AcrB function, we conducted site directed mutagenesis and discovered a key residue, R780. Although R780K was partially functional, all other R780 mutants tested were completely nonfunctional. Replacement of R780 by other residues disrupted trimer association. However, a decrease of trimer stability was not the lone cause for the observed loss of activity, because the activity loss could not be restored by strengthening trimer interaction. Using both heat and chemical denaturation methods, we found that the mutation decreased protein stability. Finally, we identified a repressor mutation, M774K, through random mutagenesis. It restored the activity of $AcrB_{R780A}$ to a level close to that of the wild-type protein. To examine the mechanism of activity restoration, we monitored denaturation of $AcrB_{R780A/M774K}$ and found that the repressor mutation improved protein stability. These results suggest that R780 is critical for AcrB stability. When R780 was replaced by Ala, the protein retained the overall structure, still trimerized in the cell membrane, and interacted with AcrA. However, local structural rearrangement might have occurred and lead to the decrease of protein stability and loss of substrate efflux activity.

The AcrAB−TolC complex in *Escherichia coli* is one of the most extensively studied examples of multidrug efflux pumps.[1] This large protein complex contains a trimeric inner membrane transporter AcrB, a trimeric outer membrane channel TolC, and three or six molecules of the membrane fusion protein AcrA.[2,3] Although all three proteins are critical for drug efflux, AcrB is the engine that drives the conformational change required by substrate transport through harvesting the energy from the influx of protons across the inner membrane. This delicate molecular machine functions as a homotrimer. Although each subunit contains independent substrate translocation and proton relay pathways, the function of subunits in a trimer is coupled.[4] In addition, substrates enter the efflux complex from portals in the periplasmic domain of AcrB.[5−8] Therefore, AcrB determines the substrate specificity of efflux. Since the publication of the first crystal structure of AcrB by Murakami et al. in 2002, more than 20 crystal structures of AcrB with or without bound substrates have been deposited into the Protein Data Bank.[9] On the basis of results from many experimental and computational studies, much has been learned about the function of AcrB and drug efflux through the AcrAB−TolC pump. A conformational cycling mechanism resembling the movement of a peristaltic pump has first been proposed on the basis of asymmetric AcrB trimer structures in 2006.[10,11] In the asymmetric trimer structure, only one subunit in each trimer binds tightly to a drug molecule. The different conformations of subunits in a trimer are designated as loose (or access), tight (or binding), and open (or extrusion) states, respectively. These structures have been proposed to represent different stages that a subunit cycles through during substrate transport.[7]

Trimerization is required for AcrB function. In addition to the structural requirement to interface with the trimeric outer membrane channel TolC, the functions of subunits in a trimer are coupled.[4] AcrB function is very sensitive to changes of trimer stability. In an effort to understand the trimerization process of AcrB, we have previously identified a mutant,

Received: April 10, 2013
Revised: September 4, 2013
Published: September 5, 2013

   dx.doi.org/10.1021/bi400452v | *Biochemistry* 2013, 52, 6790−6796

$AcrB_{P223G}$, that had little residual activity.[12] P223 is a highly conserved residue located close to the tip of a long protruding loop that is critical to intersubunit interaction during trimerization. We have established that $AcrB_{P223G}$ remained well folded, and the function loss could be largely restored by stabilizing the trimer through the introduction of an intersubunit disulfide bond between V225C and A777C.[12] These cysteines form an intersubunit disulfide bond without compromising drug efflux activity when introduced into wild-type AcrB.[12,13] The introduction of these mutations and the subsequent formation of a disulfide bond lead to a significant recovery of activity in $AcrB_{P223G}$.

In a survey of molecular interactions involving P223, we identified a residue from the neighboring subunit that is critical for AcrB function, R780. We found that the replacement of R780 by all residues tested except for Lys completely aborted the function of AcrB. Although the mutation clearly disrupted trimer association, the function loss could not be restored by stabilizing the trimer, which is different from the case of $AcrB_{P223G}$. Through random mutagenesis, we identified a repressor mutant in which M774 was replaced by Lys. The side chains of M774 and R780 are in close proximity in the crystal structure of AcrB, suggesting that a positive charge is important at this specific location. To determine the mechanism of activity loss in R780A and restoration by M774K, we conducted detailed characterization of $AcrB_{R780A}$ and $AcrB_{R780A/M774K}$.

MATERIALS AND METHODS

Site-Directed Mutagenesis, Expression, Purification, Activity Assay, and Expression Level Measurement. Site-directed mutagenesis was conducted using the QuikChange mutagenesis kit following the manufacturer's protocol (Agilent Technologies, Inc., Clara, CA). AcrB and its mutants were expressed and purified as described.[14] AcrB drug efflux activity was measured by recording the minimum inhibitory concentration (MIC) of an *acrB* gene knockout strain (BW25113Δ*acrB*) transformed with plasmid encoded AcrB or its mutant using agar plates as described.[15,16]

Circular Dichroism (CD) Spectroscopy, Disulfide Trapping, and Blue Native (BN) Polyacrylamide Gel Electrophoresis (PAGE) Analysis. CD spectra were collected as described.[14] Disulfide trapping was performed as described.[14,17] Briefly, protein expression was conducted under the basal condition without induction. The cell pellet from an overnight culture was resuspended in a lysis buffer containing 30 mM iodoacetamide (IAM) and sonicated on ice. The cell lysate was centrifuged, and the pellet was collected. Membrane proteins were extracted using a Tris buffer containing 1% Triton and 10 mM IAM. AcrB was purified from the detergent extract using metal affinity chromatography. IAM (10 mM) was present throughout the purification process. After elution, maleimide and sodium dodecyl sulfate (SDS) were immediately added to protein samples to further block any residual free Cys. Proteins were precipitated using trichloroacetic acid and resolubilized in a buffer containing SDS. Dithiothreitol (DTT) was used to reduce disulfide bond in AcrB. Finally, *N*-(5-fluoresceinyl)maleimide was added immediately to label newly reduced free thiol groups. For the internal positive control, the protein was purified and labeled similarly except that no IAM was used during the process. For the internal negative control, the protein was purified and labeled similarly except that no DTT was used to reduce disulfide bond. These controls, corresponding to 100% or no disulfide bond, respectively, were used to evaluate the level of disulfide bond formation in the corresponding sample. The labeled samples were analyzed using SDS-PAGE on 8% gels. Fluorescence image was taken using the MiniVisionary gel documentation system (FOTODYNE Inc., Hartland, WI) under UV light. The same gel was then stained using Coomassie blue stain, and the image of the gel was taken again under normal white light.

BN-PAGE was performed as described with minor modification.[18] Briefly, blue native loading buffer was added into freshly purified wild-type AcrB, $AcrB_{P223G}$, or $AcrB_{R780A}$ at a final concentration of 0.1 M 6-aminoocaproic acid, 10 mM Bis−Tris−HCl, 6% sucrose, 1% Coomassie Brilliant Blue G-250, pH 7.0. Protein samples were loaded to a 4−20% gradient polyacrylamide gel (Bio-Rad, Hercules, CA). Electrophoresis was performed using a cathode running buffer containing 50 mM tricine, 7.5 mM imidazole, 0.02% Coomassie Brilliant Blue G-250 (pH 7.0), and anode buffer with 25 mM imidazole (pH 7.0) in the 4 °C refrigerator at 15 mA for 2 h. The protein bands were visualized with Coomassie blue stain and analyzed using ImageJ (NIH).[19]

Fluorescence Spectroscopy. Fluorescence emission spectra of wild-type and mutant AcrB were collected using a LS-55 fluorescence spectrometer (PerkinElmer, Inc., Waltham, MA) at the excitation wavelength of 280 nm. Wavelength scans were performed at 20 °C. Heat denaturation was monitored with excitation and emission wavelengths of 280 and 340 nm, respectively. Chemical denaturation in SDS was monitored at the same excitation and emission wavelengths at 20 °C.

Chemical Cross-Linking of AcrA and AcrB. Chemical cross-linking was performed as described with minor modifications.[20] Briefly, plasmid pQE70-AcrB, pQE70-$AcrB_{P223G}$, or pQE70-$AcrB_{R780A}$ was transformed into BW25113Δ*acrB* for protein expression. A single colony was picked from a freshly transformed plate and grown with shaking at 37 °C in 3 mL of Lysogeny broth (LB) medium containing 100 μg/mL ampicillin for 12 h. Two milliliters of this cell culture was used to inoculate 200 mL of LB medium containing 100 μg/mL ampicillin. The culture was grown to an OD600 of 0.7. Cells were harvested by centrifugation at 5000*g* for 10 min. The cell pellet was resuspended in 10 mL of cross-linking buffer (20 mM sodium phosphate, 100 mM NaCl, pH 7.2), and the solution was incubated with 0.4 mM dithiobis succinimidyl propionate (DSP) at 37 °C for 30 min. After being quenched with 20 mM Tris, cells were collected from the solution and resuspended in a lysis buffer (20 mM Tris−HCl, 100 mM NaCl, pH 8.0). Cells were lysed through sonication on ice and centrifuged at 15 000*g* for 20 min at 4 °C. The cell pellet was resuspended in an extraction buffer (20 mM Tris−HCl, 100 mM NaCl, 1% Trition X-100, pH 8.0) and incubated with shaking for 2 h at 4 °C followed by centrifugation at 15 000*g* for 30 min at 4 °C. AcrB and cross-linked complexes were purified from the supernatant using Ni-NTA resin (Qiagen, Huntsville, AL). The eluted protein was incubated with 16 mM dithiothreitol for 30 min before it was resolved on 10% SDS-PAGE followed by immunobloting with polyclonal anti-AcrA or anti-AcrB antibodies as the primary antibodies and an alkaline phosphatase-conjugated anti-rabbit antibody (Abcam, Cambridge, MA) as the secondary antibody. The protein−antibody conjugates were detected after staining using nitroblue tetrazolium chloride and 5-bromo-4-chloro-3′-indolyl phosphate *p*-toluidine.

dx.doi.org/10.1021/bi400452v | *Biochemistry* 2013, 52, 6790−6796

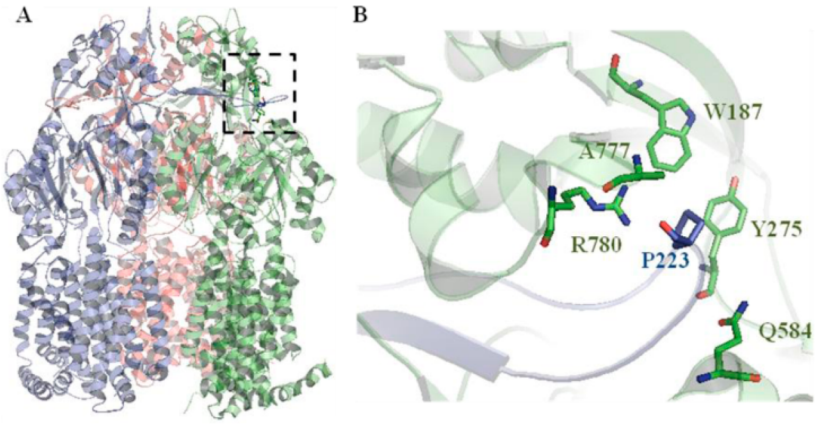

Figure 1. Structure of AcrB. (A) AcrB trimer with each subunit color coded (Protein Data Bank ID 2HRT[11]). (B) Zoom-in view of the box in (A) with residues interacting with P223 highlighted.

For the negative control, we cloned *acrA* gene followed by a stop codon into the pET-22b vector between the restriction sites *Nde*I and *Xho*I. The resultant AcrA did not have a His tag. Point mutations were introduced using the Qickchange Site-direct Mutagenesis Kit (Agilent Technologies, Inc., Clara, CA) to create $AcrA_{Q237D}$ and $AcrA_{Q237K}$. Plasmid-encoded AcrA was co-transformed with plasmid pBAD33-AcrB or pBAD33-$AcrB_{R780A}$ into strain AG100A (AG100 Δ*acrAB::kan*). Cells were cultured to an OD600 of 0.6 before expression of AcrA was induced by the addition of 0.5 mM isopropyl β-D-1-thiogalactopyranoside (IPTG). Four hours after induction, cells were collected and processed as described above.

Random Mutagenesis. Error prone PCR was performed using a GeneMorph II EZClone Domain Mutagenesis Kit following the manufacturer's instruction (Agilent Technologies, Inc., Clara, CA). Plasmid pQE-$AcrB_{R780A}$ was used as the template in the PCR reaction with two pairs of primers. The first set of primers is 5′-ATGCCTAATTTCTTTATCGAT-CGC-3′ (forward) and 5′-AACGGCGTGGTG TCGTATGG-3′ (backward), which amplified the segment between residue Met1 and Pro331. The second set of primers is 5′-CGT-TGAT-CCTG-ACTC CAGCTC-3′ (forward) and 5′- ATC-GAC-CAG-CTC-TCGTA CAG-3′ (backward), which amplified the segment between residue Leu486 and Ser896. PCR products were purified after gel electrophoresis. Next, 500 ng of each PCR product was used as a pair of mega-primers to conduct whole plasmid PCR using plasmid pQE70-$AcrB_{R780A}$ as the template. Finally, DpnI was added to digest the template. Products from the whole plasmid PCR were purified after gel electrophoresis and transformed into BW25113Δ*acrB*. Cells were plated on LB agar plates containing 8 μg/mL erythromycin. After incubation overnight, colonies were picked and cultured. Plasmids were extracted and retransformed into fresh BW25113Δ*acrB* competent cells to reconfirm the result with a drug susceptibility test. Confirmed plasmids were then sequenced to identify the site of suppressor mutation.

RESULTS

Alanine Scanning Studies of Residues Making Intersubunit Interactions with P223. Because the replacement of P223 by other residues led to the disruption of AcrB trimer stability and subsequent loss of efflux activity, we conducted an Ala-scanning experiment to identify critical residues in the neighboring subunit that interact with P223. According to the crystal structure, P223 from one subunit is in close proximity to the side chains of several residues from the neighboring subunit, including W187, Y275, Q584, A777, and R780 (Figure 1). Because $AcrB_{P223G}$ is largely nonfunctional, we expect that mutations introduced to replace its critical binding partner would have similar effects on AcrB function. These five residues were individually replaced with Ala, and the efflux activities of the resultant mutants were examined using a drug susceptibility assay (Table 1). Plasmid encoding wild-type AcrB and the empty pQE70 vector were used as positive and negative controls, respectively. $AcrB_{Y275A}$ and $AcrB_{Q584A}$ were fully active while $AcrB_{W187A}$ was partially active. Remarkably, $AcrB_{R780A}$ completely lost its activity. In the crystal structure of AcrB, the side chain of R780 is within hydrogen bond distance with the backbone carbonyl oxygen of P223. Replacement of R780 by Ala could have eliminated this interaction and therefore disrupted trimer association. To further probe the mechanism of function loss in $AcrB_{R780A}$, we replaced R780 with other residues of various charge, polarity, and length to create $AcrB_{R780M}$, $AcrB_{R780Q}$, and $AcrB_{R780K}$. $AcrB_{R780M}$ and $AcrB_{R780Q}$ were also completely nonfunctional, while $AcrB_{R780K}$ maintained a low level of function (Table 1). This result

Table 1. MIC of BW25113Δ*acrB* Transformed with Plasmid Encoding Indicated AcrB Constructs[a]

	MIC (μg/mL)				
plasmids	Aci	Ery	Nov	R6G	TPP
pQE70-AcrB	160	80	160	320	640
pQE70	10	2.5	5	5	5
pQE70-$AcrB_{W187A}$	80	40	160	320	160
pQE70-$AcrB_{Y275A}$	160	80	160	320	640
pQE70-$AcrB_{Q584A}$	160	80	160	320	640
pQE70-$AcrB_{R780A}$	10	2.5	5	5	5
pQE70-$AcrB_{R780K}$	20	20	40	40	20
pQE70-$AcrB_{R780M}$	10	2.5	5	5	5
pQE70-$AcrB_{R780Q}$	10	2.5	5	5	5
pQE70-$AcrB_{R780A/V225C/A777C}$	10	2.5	5	5	5
pQE70-$_{CL}AcrB_{V225C/A777C}$	160	80	160	320	640
pQE70-$_{CL}AcrB_{M774K}$	160	80	160	320	640
pQE70-$_{CL}AcrB_{M774R}$	160	80	160	320	640
pQE70-$_{CL}AcrB_{M774R/R780A}$	160	40	160	320	320
pQE70-$_{CL}AcrB_{M774K/R780A}$	160	40	160	320	320

[a]Drugs tested were acriflavine (Aci), erythromycin (Ery), novobiocin (Nov), rhodamine 6G (R6G), and tetraphenylphosphonium (TPP).

dx.doi.org/10.1021/bi400452v | *Biochemistry* 2013, 52, 6790−6796

suggested that a positive charge at this position might be critical for function, although no negatively charged residue could be found within the ionic interaction distance to R780 in the trimer structure.

To confirm that the decrease in activity was not a result of variation in protein expression due to mutation, we measured the expression level of each mutant. Each plasmid encoding a mutant was transformed into strain BW25113Δ*acrB* for expression under the basal condition. Protein levels in the extracted membrane vesicles were then evaluated with Western blot analysis using an anti-AcrB antibody (Figure 2A). There

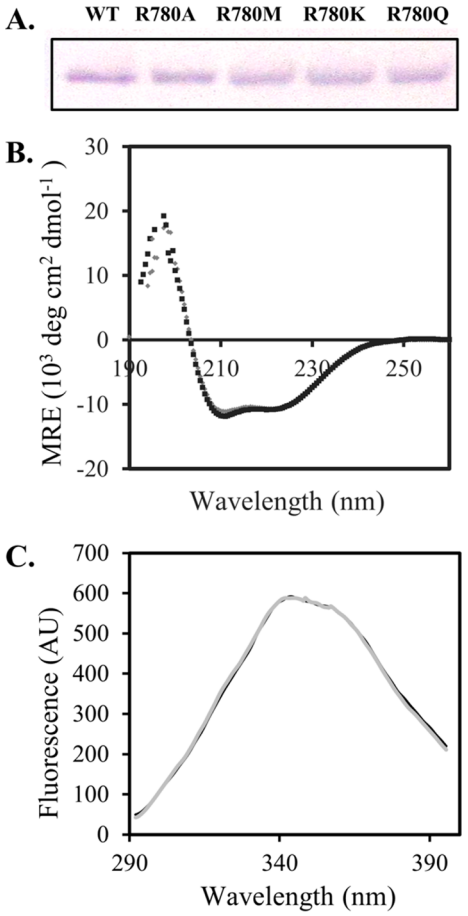

Figure 2. Characterization of R780 mutants. (A) The expression levels of wild type (WT) and mutants were comparable as revealed by the Western blot analysis. (B) Near-UV CD spectra of WT AcrB (black) and $AcrB_{R780A}$ (gray) superimposed well onto each other, indicating the two proteins had similar secondary structure contents. (C) Fluorescence spectra of WT AcrB (black) and $AcrB_{R780A}$ (gray) were similar.

was no significant difference between expression levels of wild-type AcrB and those of the mutants, indicating that the observed loss of activity was not a result of decreased protein expression.

Structure Characterization of $AcrB_{R780A}$. To evaluate the effect of mutation on protein structure, $AcrB_{R780A}$ was purified and characterized using CD and fluorescence spectroscopy and disulfide trapping. The CD spectra of $AcrB_{R780A}$ overlapped with that of wild-type AcrB (Figure 2B), indicating the secondary structures of two proteins were similar. The mutation did not have an observable effect on the intrinsic fluorescence spectrum either (Figure 2C).

The tertiary structure of $AcrB_{R780A}$ was investigated using a disulfide trapping method as previously described.[14,17] Briefly, the two intrinsic Cys in the AcrB sequence were first replaced by Ala to create Cys-less (CL) AcrB ($_{CL}$AcrB), which has been shown by several studies to be fully functional.[21] The R780A mutation was then introduced to create $_{CL}AcrB_{R780A}$. Next, a series of five Cys pairs, including T44C−T91C, M184C−V771C, V32C−I390C, T199C−T749C, and A216C−I234C, were introduced into $_{CL}$AcrB and $_{CL}AcrB_{R780A}$ to probe local conformational change. These Cys pair reporters distributed throughout the periplasmic domain of AcrB (Figure 3A). All five Cys pairs formed disulfide bonds in $_{CL}$AcrB, consistent with our earlier observations (Figure 3B).[12,17] The levels of disulfide bond formation were evaluated by comparing the intensities of fluorescent bands with those of the internal positive and negative controls as described in the Materials and Methods. Although small differences in the level of disulfide bond could be observed for the C184−C771 pair, overall the disulfide bond formed to similar levels in $_{CL}$AcrB and $_{CL}AcrB_{R780A}$, indicating that the R780 to Ala mutation did not cause a significant change of the overall tertiary structure of the protein.

Next, the quaternary structure of freshly purified $AcrB_{R780A}$ was determined using BN-PAGE (Figure 4A). Freshly purified wild-type AcrB and $AcrB_{P223G}$ were also loaded on the same gel for comparison. Wild-type AcrB migrated as a trimer while most $AcrB_{P223G}$ and $AcrB_{R780A}$ migrated as monomers, indicating that R780 was involved in the oligomerization of the protein as expected. The band intensities for the proteins were quantified, which revealed that $AcrB_{R780A}$ had slightly less trimer content than that for $AcrB_{P223G}$ (Figure 4B).

In an earlier study, we found that the function loss caused by P223G mutation could be partially restored through the introduction of an intersubunit disulfide bond A777C/V225C, and the presence of DTT in the culture aborted this recovery effect, suggesting that P223G mutation leads to function loss mainly through disrupting trimerization.[12] Similarly, we introduced A777C/V225C into $_{CL}AcrB_{R780}$. Membrane vesicles extracted from BW25113Δ*acrB* expressing $_{CL}AcrB_{R780A/V225C/A777C}$ were analyzed using Western blot (Figure 4C). Similar as previously reported for $_{CL}AcrB_{P223G/V225C/A777C}$, $_{CL}AcrB_{R780A/A777C/V225C}$ also formed a covalent trimer. In the absence of DTT, a clear trimer band could be observed in SDS-PAGE, indicating that the mutant $AcrB_{R780A}$ still trimerized *in vivo*. However, unlike in the case of the P223G mutation, the function of $AcrB_{R780A}$ was not restored. For all substrates tested, the minimum inhibitory concentration (MIC) value of BW25112Δ*acrB* containing $_{CL}AcrB_{R780A/V225C/A777C}$ was the same as the MIC value of the strain containing $AcrB_{R780A}$ (Table 1).

Chemical Cross-Linking with AcrA. Another mechanism that may affect efflux is through disrupting the interaction between AcrB and its partner proteins AcrA and TolC. The direct interaction between AcrA and AcrB has been well established.[20] To examine the effect of mutation on the interaction between AcrB and AcrA *in vivo*, a chemical cross-linking experiment was performed using cross-linker DSP. We examined the cross-linking of wild-type AcrB and $AcrB_{R780A}$ with both wild-type AcrA and two AcrA mutants that contained either the Q237D or Q237K mutations (Figure 5). Although the structure of the AcrA−AcrB complex is not yet available, their potential interface has been the subject of many studies.[22−25] In a study on close AcrA−AcrB homologues MexA−MexB, mutation of R221 in MexA, corresponding to

dx.doi.org/10.1021/bi400452v | *Biochemistry* 2013, 52, 6790−6796

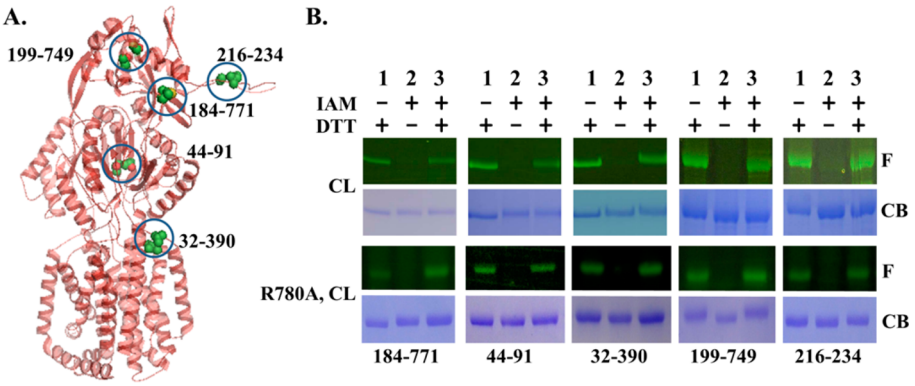

Figure 3. Disulfide trapping analysis of AcrB tertiary structure. (A) Locations of reporter Cys pairs in the structure of AcrB were highlighted using blue circles and green ball-and-stick models. Residues replaced by Cys were marked. (B) Thiol-specific fluorescent labeling of Cys pairs introduced into Cys-less AcrB background or $AcrB_{R780A}$ background (R780A, CL). Lanes 1 and 2 are the positive and negative controls, respectively. For each sample, a fluorescent image was first taken (F) and then the gel was stained using Commassie Brilliant Blue (CB).

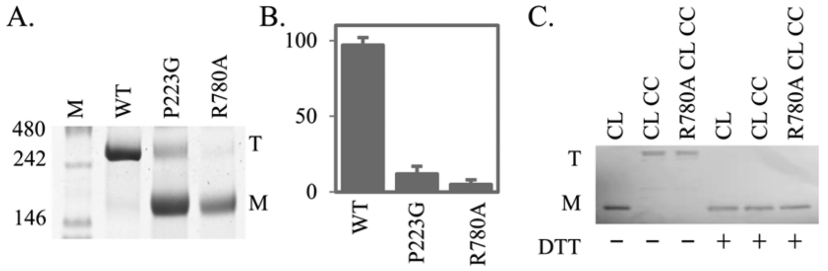

Figure 4. Quaternary structure analysis. (A) Representative BN-PAGE gel image of freshly purified $AcrB_{WT}$, $AcrB_{R780A}$, and $AcrB_{P223G}$. (B) Percentage of AcrB trimer content for each sample was calculated from BN-PAGE analysis. Average value and standard deviation from three repeats were shown. (C) Representative Western blot image of membrane vesicles extracted from BW25113Δ*acrB* expressing $_{CL}AcrB$ (CL), $_{CL}AcrB_{V225C/A777C}$ (CL CC), or $_{CL}AcrB_{R780A/V225C/A777C}$ (R780A CL CC), with or without 4 mM DTT.

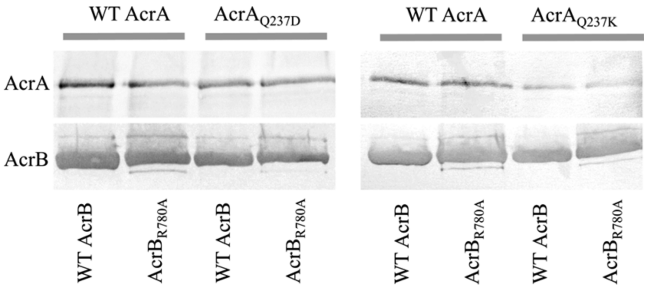

Figure 5. Chemical cross-linking of AcrB and AcrA. After cross-linking, samples were purified using metal affinity chromatography, reduced using DTT, and resolved on 10% SDS-PAGE. Representative images of anti-AcrA and anti-AcrB Western blots were shown, which revealed that similar amounts of wild-type AcrA, $AcrA_{Q237D}$, or $AcrA_{Q237K}$ were cross-linked with wild-type AcrB and $AcrB_{R780A}$.

Q237 in AcrA, disrupts the interaction between MexA and MexB.[26] Therefore, we expected that mutation of Q237 might affect the interaction between AcrA and AcrB and intended to use $AcrA_{Q237D}$ and $AcrA_{Q237K}$ as negative controls. There was no significant difference between the level of AcrA cross-linked with $AcrB_{R780A}$ and wild-type AcrB. Mutation of AcrA Q237 into Asp did not have an observable effect on the interaction with either wild-type AcrB or $AcrB_{R780A}$. The more drastic mutation, Q237K, did reduce the level of AcrA cross-linked with both AcrB constructs. These results indicated that $AcrB_{R780A}$ interacted with AcrA in a similar fashion as wild-type AcrB did.

Repressor Mutations That Restore the Function of R780A. We conducted random mutagenesis experiments to identify mutations that restore the function of $AcrB_{R780A}$. We focused our search on the periplasmic domain, which is composed of the two long periplasmic loops between residues L38 to T330 and S561 to G870. Through multiple rounds of experiment, only one repressor mutation was repeatedly identified, M774K. The mutation restored the function of $AcrB_{R780A}$ to a level close to the activity of the wild-type protein (Table 1). The activity of $AcrB_{R780A/M774K}$ double mutant was even higher than the activity of $AcrB_{R780K}$. Because M774K could restore the function of $AcrB_{R780A}$, we have also checked the effect of M774R mutation and found it was equally as effective in recovering the function loss (Table 1). On the basis of the crystal structure, the side chain of M774, especially the terminal of it, is within close proximity to the guanidinium group in the side chain of R780. This result again indicated that a positive charge at this position is critical for the structure and function of AcrB.

Protein Stability Analyses. To further investigate the mechanism of activity loss in $AcrB_{R780A}$ and recovery in $AcrB_{R780A/M774K}$, we compared the thermal stabilities of these two mutants with that of wild-type AcrB. First, protein denaturation upon an increase of temperature was monitored using CD and recording the ellipiticity at 222 nm (Figure 6A). Here, the unfolding of protein secondary structure, especially the α-helix, was monitored. The spectra of wild-type AcrB and $AcrB_{R780A}$ superimposed well. Next, heat denaturation was monitored using fluorescence emission at 340 nm while excited at 280 nm (Figure 6B). Because temperature is known to affect

dx.doi.org/10.1021/bi400452v | *Biochemistry* 2013, 52, 6790−6796

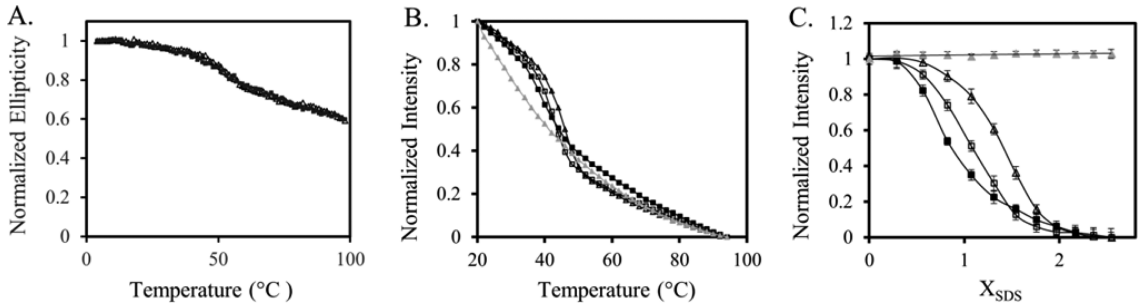

Figure 6. Stability analyses of wild-type and mutant AcrB. (A) Heat denaturation of wild type (open triangles) and $AcrB_{R780A}$ (filled squares) monitored at 222 nm using CD. (B) Heat denaturation of wild type (open triangles), $AcrB_{R780A}$ (filled squares), and $AcrB_{R780A/M774K}$ (open squares) monitored using fluorescence emission. Amino acid L-tryptophan (gray triangles) was used as a control for nondenaturation related fluorescence intensity change. (C) SDS denaturation of wild type (open triangles), $AcrB_{R780A}$ (filled squares), and $AcrB_{R780A/M774K}$ (open squares) monitored using fluorescence emission. Amino acid L-tryptophan (gray triangles) was used as a control for nondenaturation related fluorescence intensity change.

fluorescence intensity, we used amino acid L-tryptophan as a control for nondenaturation related temperature effect (gray triangles). Fluorescence of L-tryptophan decreased gradually with temperature. The melting curve of $AcrB_{R780A}$ (filled squares) was quite different from that of the wild-type protein (open triangles). A clear transition could be observed at ~45 °C for wild-type AcrB. The transition of $AcrB_{R780A}$ was not as clear, and unfolding started at a lower temperature. The introduction of the repressor mutation M774K partially restored the shape of the melting curve to reveal a clear transition at ~42 °C. Finally, unfolding of AcrB was observed in the presence of SDS. SDS has been used in several studies to unfold membrane proteins.[27] The intrinsic fluorescence of AcrB was used to monitor protein unfolding (Figure 6C). As a control of potential detergent effect not related to protein unfolding, the amino acid L-tryptophan was also included in the study (gray triangles). The addition of SDS in the concentration range tested did not have an effect on L-tryptophan fluorescence. The unfolding curves of three proteins were clearly different, with the stability decreased from wild-type AcrB, to $AcrB_{R780A/M774K}$, and finally to $AcrB_{R780A}$. In addition to the difference in half point SDS molar ratios at which 50% of protein unfolded, the slopes of the curves were also different. The denaturation curves of wild-type AcrB and $AcrB_{R780A/M774K}$ were steeper than the curve of $AcrB_{R780A}$. Protein unfolding for the first two proteins occurred in a narrower SDS concentration range, indicating that their internal structures were more ordered and well-packed.

DISCUSSION

A functionless mutant, R780A, was identified in a survey of intersubunit binding partners of P223 in the AcrB trimer. It was the site with the least tolerance to mutations among all sites we have tested at the intersubunit interface.[12,28] Although most mutations introduced at various sites on the intersubunit interface retained at least some residual drug efflux activity, all R780 mutants tested, except for R780K, were completely functionless. Similar as for $AcrB_{P223G}$, the CD spectra, fluorescence spectra, and disulfide bond trapping experiments revealed that the secondary and tertiary structures of $AcrB_{R780A}$ were similar to the structures of wild-type AcrB. Purified $AcrB_{R780A}$ migrated predominantly as monomers in BN-PAGE, indicating that the mutation did decrease the affinity of trimer association as expected. However, although the function loss in $AcrB_{P223G}$ can be largely restored through the introduction of an intersubunit disulfide bond to compensate for the loss of trimer stability, a similar effect was not observed when the same disulfide bond was introduced into $AcrB_{R780A}$. $AcrB_{R780A/V225C/A777C}$ remained functionless. In addition, the R780A mutation did not appear to affect the interaction between AcrA and AcrB according to the result of co-expression and chemical cross-linking. We acknowledge that the cross-linking experiment had its limitations. It could not differentiate between functionally relevant interactions from unspecific background interaction due to the presence of both proteins in the sample.

Among R780 mutants created in this study, only the conservative mutation R780K maintained partial activity. Interestingly, the function loss caused by the R780A mutation could be largely restored by an additional M774K or M774R mutation (Table 1). The side chains of M774 and R780 are in close proximity in the protein structure. These results strongly support the conclusion that a positive change is required at this specific site for AcrB to operate. According to the crystal structure of AcrB trimer, there is no negatively charged side chain within the distance of ionic interaction of the positive charge on R780. A likely interaction partner of the R780 positive charge is the carbonyl group of P223 from the neighboring subunit, and possibly also the nearby carbonyl group of T222. The charge is more focused at the side chain primary amino group in Lys as compared to the distributed charge over the guanidinium group in Arg, which may help to explain the partial activity in the R780K mutant.

We compared the thermal stability of wild-type AcrB, $AcrB_{R780A}$, and the repressor mutant $AcrB_{R780A/M774K}$. No difference in stability could be observed between wild-type AcrB and $AcrB_{R780A}$ when the unfolding of secondary structure was monitored using CD. Residual helical structure could be observed even when the proteins were heated to 98 °C, which is consistent with previous observations that transmembrane helices in helical membrane proteins are very stable and a portion of which exists even in the unfolded stage.[29] However, a clear difference could be observed when intrinsic fluorescence was monitored upon the increase of temperature. $AcrB_{R780A}$ was clearly less stable than wild-type AcrB. This observation was confirmed by chemical denaturation using SDS. The R780A mutation not only decreased the melting point but also affected the slope of the denaturation curves, revealing the disruption effect of the internal packing of AcrB subunit structure.[30] Therefore, we conclude that R780A mutation disrupted the

dx.doi.org/10.1021/bi400452v | Biochemistry 2013, 52, 6790−6796

function of AcrB by disturbing the local conformation and reducing the thermal stability of AcrB. The observed decrease of trimer affinity is not the direct cause of activity loss but rather a consequence of local structure change due to the mutation.

AUTHOR INFORMATION

Corresponding Author

*Y. Wei. 305 Chemistry-Physics Building, University of Kentucky, Lexington, KY 40506-0055. Telephone: (859) 257-7085. Fax: (859) 323-1069. E-mail: yinan.wei@uky.edu.

Funding

This research is supported by the National Science Foundation (MCB 1158036, Y.W.) and Kentucky NASA EPSCoR program.

Notes

The authors declare no competing financial interest.

ACKNOWLEDGMENTS

We thank Dr. Hiroshi Nikaido for the kind gift of *E. coli* strain AG100A.

ABBREVIATIONS

BN-PAGE, blue native polyacrylamide gel electrophoresis; MIC, minimum inhibitory concentrations; Ery, erythromycin; Nov, novobiocin; R6G, rhodamine 6G; TPP, tetraphenylphosphonium; SDS-PAGE, sodium dodecyl sulfate polyacrylamide gel electrophoresis; DDM, *n*-dodecyl β-D-maltoside; CD, circular dichroism; IAM, iodoacetamide; DTT, dithiothreitol

REFERENCES

(1) Nikaido, H., and Pages, J. M. (2012) Broad-specificity efflux pumps and their role in multidrug resistance of Gram-negative bacteria. *FEMS Microbiol. Rev. 36*, 340−363.

(2) Blair, J. M., and Piddock, L. J. (2009) Structure, function and inhibition of RND efflux pumps in Gram-negative bacteria: An update. *Curr. Opin. Microbiol. 12*, 512−519.

(3) Nikaido, H., and Takatsuka, Y. (2009) Mechanisms of RND multidrug efflux pumps. *Biochim. Biophys. Acta 1794*, 769−781.

(4) Takatsuka, Y., and Nikaido, H. (2009) Covalently linked trimer of the AcrB multidrug efflux pump provides support for the functional rotating mechanism. *J. Bacteriol. 191*, 1729−1737.

(5) Husain, F., and Nikaido, H. (2010) Substrate path in the AcrB multidrug efflux pump of *Escherichia coli*. *Mol. Microbiol. 78*, 320−330.

(6) Bohnert, J. A., Schuster, S., Seeger, M. A., Fahnrich, E., Pos, K. M., and Kern, W. V. (2008) Site-directed mutagenesis reveals putative substrate binding residues in the *Escherichia coli* RND efflux pump AcrB. *J. Bacteriol. 190*, 8225−8229.

(7) Pos, K. M. (2009) Drug transport mechanism of the AcrB efflux pump. *Biochim. Biophys. Acta 1794*, 782−793.

(8) Seeger, M. A., Diederichs, K., Eicher, T., Brandstatter, L., Schiefner, A., Verrey, F., and Pos, K. M. (2008) The AcrB efflux pump: conformational cycling and peristalsis lead to multidrug resistance. *Curr. Drug Targets 9*, 729−749.

(9) Murakami, S., Nakashima, R., Yamashita, E., and Yamaguchi, A. (2002) Crystal structure of bacterial multidrug efflux transporter AcrB. *Nature 419*, 587−593.

(10) Murakami, S., Nakashima, R., Yamashita, E., Matsumoto, T., and Yamaguchi, A. (2006) Crystal structures of a multidrug transporter reveal a functionally rotating mechanism. *Nature 443*, 173−179.

(11) Seeger, M. A., Schiefner, A., Eicher, T., Verrey, F., Diederichs, K., and Pos, K. M. (2006) Structural asymmetry of AcrB trimer suggests a peristaltic pump mechanism. *Science 313*, 1295−1298.

(12) Yu, L., Lu, W., and Wei, Y. (2011) AcrB trimer stability and efflux activity, insight from mutagenesis studies. *PLoS ONE 6*, e28390.

(13) Seeger, M. A., von Ballmoos, C., Eicher, T., Brandstatter, L., Verrey, F., Diederichs, K., and Pos, K. M. (2008) Engineered disulfide bonds support the functional rotation mechanism of multidrug efflux pump AcrB. *Nat. Struct. Mol. Biol. 15*, 199−205.

(14) Lu, W., Zhong, M., and Wei, Y. (2011) Folding of AcrB Subunit Precedes Trimerization. *J. Mol. Biol. 411*, 264−274.

(15) Lu, W., Chai, Q., Zhong, M., Yu, L., Fang, J., Wang, T., Li, H., Zhu, H., and Wei, Y. (2012) Assembling of AcrB trimer in cell membrane. *J. Mol. Biol. 423*, 123−134.

(16) Wiegand, I., Hilpert, K., and Hancock, R. E. (2008) Agar and broth dilution methods to determine the minimal inhibitory concentration (MIC) of antimicrobial substances. *Nat. Protoc. 3*, 163−175.

(17) Lu, W., Zhong, M., and Wei, Y. (2011) A reporter platform for the monitoring of in vivo conformational changes in AcrB. *Protein Pept. Lett. 18*, 863−871.

(18) Wittig, I., Braun, H. P., and Schagger, H. (2006) Blue native PAGE. *Nat. Protoc. 1*, 418−428.

(19) Abramoff, M. D., Magalhaes, P. J., and Ram, S. J. (2004) Image processing with ImageJ. *Biophoton. Int. 11*, 36−42.

(20) Zgurskaya, H. I., and Nikaido, H. (2000) Cross-linked complex between oligomeric periplasmic lipoprotein AcrA and the inner-membrane-associated multidrug efflux pump AcrB from *Escherichia coli*. *J. Bacteriol. 182*, 4264−4267.

(21) Takatsuka, Y., and Nikaido, H. (2007) Site-directed disulfide cross-linking shows that cleft flexibility in the periplasmic domain is needed for the multidrug efflux pump AcrB of *Escherichia coli*. *J. Bacteriol. 189*, 8677−8684.

(22) Krishnamoorthy, G., Tikhonova, E. B., and Zgurskaya, H. I. (2008) Fitting periplasmic membrane fusion proteins to inner membrane transporters: Mutations that enable *Escherichia coli* AcrA to function with *Pseudomonas aeruginosa* MexB. *J. Bacteriol. 190*, 691−698.

(23) Fernandez-Recio, J., Walas, F., Federici, L., Venkatesh Pratap, J., Bavro, V. N., Miguel, R. N., Mizuguchi, K., and Luisi, B. (2004) A model of a transmembrane drug-efflux pump from gram-negative bacteria. *FEBS Lett. 578*, 5−9.

(24) Higgins, M. K., Bokma, E., Koronakis, E., Hughes, C., and Koronakis, V. (2004) Structure of the periplasmic component of a bacterial drug efflux pump. *Proc. Natl. Acad. Sci. U. S. A. 101*, 9994−9999.

(25) Elkins, C. A., and Nikaido, H. (2003) Chimeric analysis of AcrA function reveals the importance of its C-terminal domain in its interaction with the AcrB multidrug efflux pump. *J. Bacteriol. 185*, 5349−5356.

(26) Nehme, D., Li, X. Z., Elliot, R., and Poole, K. (2004) Assembly of the MexABOprM multidrug efflux system of *Pseudomonas aeruginosa*: Identification and characterization of mutations in mexA compromising MexA multimerization and interaction with MexB. *J. Bacteriol. 186*, 2973−2983.

(27) Hong, H., Joh, N. H., Bowie, J. U., and Tamm, L. K. (2009) Methods for measuring the thermodynamic stability of membrane proteins. *Methods Enzymol. 455*, 213−236.

(28) Fang, J., Yu, L., Wu, M., and Wei, Y. (2013) Dissecting the function of a protruding loop in AcrB trimerization. *J. Biomol. Struct. Dyn. 31*, 385−392.

(29) Curnow, P., and Booth, P. J. (2007) Combined kinetic and thermodynamic analysis of alpha-helical membrane protein unfolding. *Proc. Natl. Acad. Sci. U. S. A. 104*, 18970−18975.

(30) Freire, E. (1995) Thermal denaturation methods in the study of protein folding. *Methods Enzymol. 259*, 144−168.